ISSN 0021-3640, JETP Letters, 2022, Vol. 116, No. 9, pp. 613–618. © The Author(s), 2022. This article is an open access publication.
Russian Text © The Author(s), 2022, published in Pis'ma v Zhurnal Eksperimental'noi i Teoreticheskoi Fiziki, 2022, Vol. 116, No. 9, pp. 592–598.

OPTICS
AND LASER PHYSICS

Simulation and Analysis of the Optical Characteristics of Cylindrical Micropillars with InAs/GaAs Quantum Dots

M. A. Bobrov[a, b, *], S. A. Blokhin[a], N. A. Maleev[a], A. G. Kuz'menkov[a], A. A. Blokhin[a], A. P. Vasil'ev[c], Yu. A. Guseva[a], M. V. Rakhlin[a], A. I. Galimov[a], Yu. M. Serov[a], S. I. Troshkov[a], V. M. Ustinov[b], and A. A. Toropov[a]

[a] *Ioffe Institute, St. Petersburg, 194021 Russia*

[b] *Peter the Great St. Petersburg Polytechnic University, St. Petersburg, 195251 Russia*

[c] *Research & Engineering Center Submicron Heterostructures for Microelectronics, Russian Academy of Sciences, St. Petersburg, 194021 Russia*

**e-mail: bobrov.mikh@gmail.com*

Received September 26, 2022; revised September 26, 2022; accepted September 26, 2022

The optical characteristics of vertical cylindrical micropillars with AlGaAs distributed Bragg reflectors and InAs/GaAs quantum dots, which are designed for the fabrication of single-photon sources, have been studied. The effect of parameters such as the inclination angle of sidewalls, partial oxidation of AlGaAs layers, and deviation of quantum dots from the central axis of a micropillar on the Purcell factor and the radiation extraction efficiency has been numerically simulated by the finite-difference time-domain method. The allowable ranges of the listed parameters have been determined for cylindrical vertical 920-nm micropillars. The comparison of the calculations performed with the refined refractive indices of the used materials at cryogenic temperatures with the measured characteristics of the fabricated micropillar structures has confirmed the adequacy of the used models.

DOI: 10.1134/S0021364022800207

Cylindrical micropillars (CMPs) with semiconductor quantum dots (QDs) underlie one of the most promising variants of the implementation of single-photon sources for future quantum cryptography systems [1] and quantum computing [2]. A basic element of CMPs is a microcylinder with a characteristic diameter of 1–4 μm, which is made of an epitaxial heterostructure with two distributed Bragg reflectors between which a GaAs micropillar including a layer of InAs/GaAs QDs with a low surface density is placed [3]. Distributed Bragg reflectors consist of alternating quarter-wave AlGaAs layers with high and low Al contents; self-organization effects in InGaAs/GaAs heterostructures were used to form QDs [4]. The optimal CMP has a strictly cylindrical shape and smooth vertical walls [5]. It is assumed that an emitting element (QD) is located at the geometric center of an optical microcavity and the radiation wavelength of the QD coincides with the resonance wavelength. Modern epitaxial equipment and careful calibration of growth parameters allow one to ensure the achievement of the designed thickness and composition of epitaxial layers, as well the positioning of the plane with QDs, with an accuracy of ~1% or better [6]. At the same time, a possible inclination of sidewalls of the microcylinder, roughness of its surface, partial local oxidation of AlGaAs layers with a high Al content, and the deviation of the emitting QD from the vertical axis of the micropillar should be taken into account when implementing CMPs with QDs [7]. It is relevant to study the effect of the listed factors on the optical characteristics of CMPs with QDs and the expected characteristics of single-photon sources based on them.

In this work, the effect of the inclination of sidewalls, partial oxidation of AlGaAs layers, and deviation of the quantum dot from the central axis of the micropillar on the main optical characteristics of CMPs functioning as single-photon sources at a wavelength of about 920 nm is numerically simulated. The experimental studies of the optical characteristics of fabricated CMPs and the calculations performed with the refined refractive indices of the used materials at cryogenic temperatures are comparatively analyzed.

We comparatively examined CMPs fabricated by means of photolithography and plasmochemical etching from heterostructures grown by molecular-beam epitaxy on GaAs substrates [8]. Heterostructures included two distributed Bragg reflectors consisting of a set of pairs of $Al_{0.9}Ga_{0.1}As$/GaAs layers each with a thickness of $\lambda/(4n)$, where λ is the resonance wavelength and n is the refractive index of the respective material. A GaAs resonance layer with a thickness of λ/n with a layer of InAs QDs with a low surface density

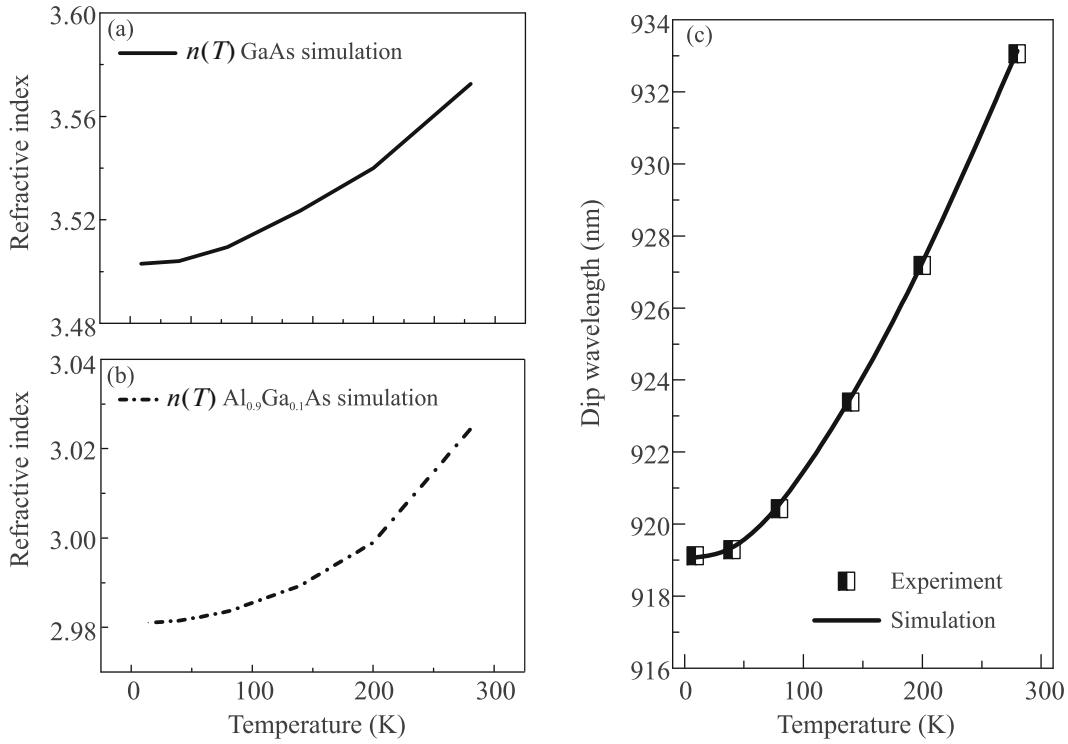

Fig. 1. (a, b) Refined temperature dependences of the refractive indices of (a) GaAs and (b) $Al_{0.9}Ga_{0.1}As$. (c) Temperature dependence of the spectral position of the fundamental mode of the planar heterostructure of the micropillar according to the (line) simulation and (half-filled squares) experiment.

(~(1–2) × 10^9 cm^{-2}) was sandwiched between distributed Bragg reflectors. The upper and lower distributed Bragg reflectors in structures under study contained 15 and 28 pairs of quarter-wave layers, respectively. The parameters of distributed Bragg reflectors were chosen in such a way as to significantly increase the spontaneous emission rate in QDs owing to the Purcell effect and to keep a sufficiently high radiation extraction efficiency [9, 10]. This design was used in all model calculations.

To compare the calculations with experimental data, we measured both spectra of optical reflection of initial planar heterostructures and microreflection spectra from individual CMPs with different inclination angles of the walls of the cylinder and different top diameters varying in different structures from 1.8 to 4.6 μm. Microreflection spectra were measured in a microscope system based on a liquid helium flow microcryostat with low-temperature three-coordinate piezoelectric stages, which ensured an adjustment accuracy of about 20 nm [8].

Efficient single-photon generation requires the cooling of the emitting CMP to cryogenic temperatures of ≤20 K. For this reason, the appropriate choice of the refractive indices of $Al_{0.9}Ga_{0.1}As$ and GaAs layers in the spectral region of interest at these temperatures is crucially important for the simulation of the parameters of CMPs. The refined temperature dependences of the refractive indices were obtained by comparing the calculations and the measured temperature dependence of the resonance wavelength in the initial planar microcavity heterostructure used to fabricate arrays of CMPs. The position of resonance was determined from the simulation of reflection spectra from the planar heterostructure by the transfer matrix method. The measured dependences could not be adequately described within the previously proposed model of the temperature dependence of refractive indices [11], which is based on the linear extrapolation of experimental data obtained near room temperature. To reproduce experimental data at cryogenic temperatures, we proposed refined polynomial temperature dependences of the refractive indices of GaAs and $Al_{0.9}Ga_{0.1}As$ layers, which are plotted in Figs. 1a and 1b.

To simulate the optical characteristics of CMPs with QDs, we numerically solved Maxwell's equations using the finite-difference time-domain method [12]. The practical implementation of this method involves the problem of the inaccurate mapping of the interface between two media to the computational grid. The staircase effect distorts the curved interface geometrically mismatched with the computational grid and thereby reduces the accuracy of calculations with the finite-difference time-domain method. To solve this problem without a significant increase in computational resources, we introduced an effective dielectric

constant near the interface between two materials [13] and approximated the single InAs QD (radiation source) by a dipole located in the central GaAs plane of the active region of the CMP between two $Al_{0.9}Ga_{0.1}As/GaAs$ distributed Bragg reflectors. To calculate reflection and transmission spectra, a detecting rectangular parallelepiped was formed around the CMP; its faces were used to determine the fractions of radiation emitted by the source in the upward, downward, and sideward directions. The determined electric and magnetic fields on detecting surfaces were transformed to the frequency representation with the discrete Fourier transform. Further, using the calculated Poynting vector as a function of time, we determined the average flux of the electromagnetic energy through each detecting surface. Dividing the determined flux by the dipole excitation pulse power, we calculated reflection and transmission spectra of interest using the proposed refined temperature dependences of the refractive indices of GaAs and $Al_{0.9}Ga_{0.1}As$ layers.

Reflection spectra of an array of CMPs were measured at a temperature of 9 K; the exact geometrical sizes and wall inclination angle were determined from scanning electron microscopy data. The spectral positions of resonance peaks corresponding to the two first modes of the micropillar (LP01 and LP02) and their dependences on the measured top diameter of the CMP were determined from the measured reflection spectra. Figure 2 shows the dependence of the spectral positions of resonance peaks corresponding to the two first modes of the CMP on the top diameter according to (squares and triangles) the experimental data obtained with a sidewall inclination angle of 3.5° and (lines) simulation with a sidewall inclination angle of (dash-dotted lines) 0° and (dashed lines) 3.5°. It is seen that the difference between the experimental data and simulation results for a sidewall inclination angle of 3.5° is less than 3%, which confirms the adequacy of the developed model.

The photon extraction efficiency (PEE), the Purcell factor F_P, and the Q factor of the micropillar are the most important optical characteristics for the application of CMPs as single-photon sources. In the calculations by the finite-difference time-domain method, the PEE was estimated as the ratio of the electromagnetic energy flux through the upper detecting surface to the total flux emitted by the dipole. The Purcell factor was determined as the ratio of the Q factor of the micropillar to the volume of its optical mode V_m with an additional coefficient according to [14]. The Q factor of the micropillar was taken as the ratio of the wavelength of the fundamental mode wavelength to the FWHM of the resonance peak.

The effect of different factors was analyzed in detail for the CMP with a diameter of 2.5 μm, which is close to the optimal value ensuring the maximum product of the PEE and the Purcell factor, which is confirmed by

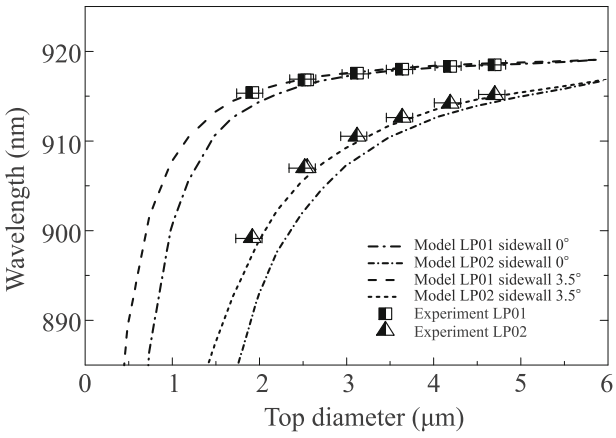

Fig. 2. Spectral positions of the resonance peaks for the first two modes LP01 and LP02 of the cylindrical micropillar versus the top diameter of the micropillar according to (squares and triangles) the experimental data obtained from the measured reflection spectra, (dash-dotted lines) the simulation of the cylindrical micropillar with vertical walls, and (dashed lines) the simulation of the cylindrical micropillar with the sidewall inclination angle of 3.5°; the long dashed and dash-dotted lines and the short dashed and dash-dotted lines correspond to the LP01 and LP02 modes, respectively.

the results reported in [15]. All calculations were performed for a working temperature of 9 K.

To evaluate the effect of the inclination of the sidewalls of the CMP on the input of the radiation from the single-photon source in an optic fiber, we analyzed the photon collection efficiency in a given aperture angle, which was calculated as the ratio of the dipole radiation power in the far field in the given aperture angle to the total radiation power emitted in the upper hemisphere. Figure 3a presents the calculated photon collection efficiency as a function of the numerical aperture for the CMP with a top diameter of 2.5 μm either (solid line) with the vertical walls or (dashed line) with a sidewall inclination angle of 3.5°. According to the corresponding measurements, the single-photon collection efficiency is the same for objectives with numerical apertures NA = 0.7 and 0.45. This conclusion is in good agreement with the calculations according to which the photon collection efficiencies for the CMP with a sidewall inclination angle of 3.5° for numerical apertures NA = 0.7 and 0.45 differ by no more than 2%.

To estimate the effect of the lateral deviation of the QD from the vertical axis of the CMP, we calculated the Purcell factor and the photon extraction efficiency for two CMPs with a top diameter of 2.5 μm, with vertical and inclined sidewalls, and with different positions of the radiation source (see Fig. 3b). It is seen that the PEE decreases by 20% when the dipole deviates by 830 and 910 nm from the vertical axis of the CMPs with the vertical sidewalls and sidewalls inclined by 3.5°, respectively. However, the require-

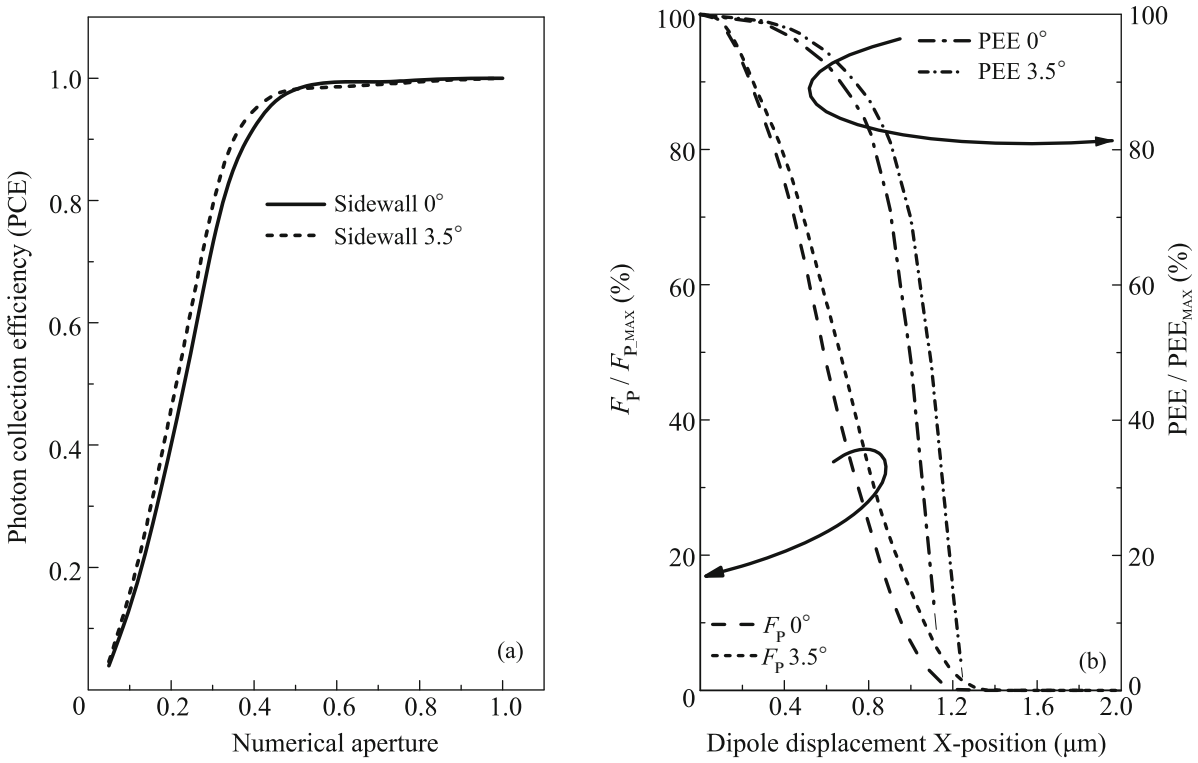

Fig. 3. Calculated optical characteristics of cylindrical micropillars with a top diameter of 2.5 μm. (a) Photon collection efficiency versus the aperture angle for (solid line) the micropillar with the vertical walls and (dashed line) the micropillar with the sidewall inclination angle of 3.5°. (b) Purcell factor and the photon extraction efficiency versus the lateral shift of the emitting dipole from the vertical axis of the cylindrical micropillar in units of the maximum values of the respective parameters at the position of the dipole exactly on the central axis of the micropillar.

ment that F_P should be no less than 80% of its maximum value imposes a more stringent constraint on the maximum allowed deviation of the emitting dipole from the central position. This deviation for the CMPs with the vertical sidewalls and sidewalls inclined by 3.5° should be no more than 350 and 400 nm, respectively. This difference is explained by an increase in the effective volume V_m of the mode of the micropillar with an increase in the inclination angle of the sidewalls of the CMP, which leads to an increase in the allowed deviation of the dipole from the vertical axis at which the Purcell factor F_P and PEE are no less than 80% of the respective maximum values. Thus, the Purcell factor F_P and PEE no less than 80% of the respective maximum values for the CMP with inclined walls and a top diameter 2.5 μm can be ensured if the QD deviates from the vertical axis of the micropillar by no more than 0.4 μm.

The fabrication of CMPs for single-photon sources can also be accompanied by the partial lateral oxidation of $Al_{0.9}Ga_{0.1}As$ layers with a high Al content in the absence of the protection of the surface. Such an uncontrolled and comparatively slow oxidation leads to the formation of an oxide layer with the refractive index close to 1.6. As a result, local regions with a large jump of the refractive index are formed near the surface of sidewalls and can be responsible for additional optical losses because of radiation scattering. To determine the effect of this process on the optical properties of CMPs under study, we simulated CMPs with $Al_{0.9}Ga_{0.1}As$ layers oxidized to 200 nm in the lateral direction from the surface of the walls of the microcylinder. A variant with the protective polyamide coating of the side surface to prevent oxidation and to ensure time-stable characteristics of single-photon sources was also simulated for comparison.

The results of calculations for the considered CMPs are summarized in Table 1. The microcylinder with perfectly vertical smooth walls was considered as an ideal CMP whose optical characteristics were compared with those of other variants. The dipole collection efficiency in the numerical aperture NA = 0.42 for the micropillar with vertical sidewalls and $Al_{0.9}Ga_{0.1}As$ layers laterally oxidized to a depth of 200 nm decreases from 74 to 67%. Simultaneously, the Purcell factor F_P increases from 11.2 to 13.6 and the wavelength of radiation decreases by 1 nm because of a decrease in V_m of the micropillar. The calculations for the structure with a sidewall inclination angle of 3.5° indicate a further decrease in the dipole collection efficiency in the numerical aperture NA = 0.42 to

Table 1. Results of the calculation of the effect of the inclination of the walls, side oxidation of AlGaAs layers and the protective coating of the cylindrical micropillar on the optical characteristics of the fundamental mode of the LP01 micropillar with a top diameter of 2.5 μm

λ (nm)	Q factor	Purcell factor F_P	Dipole collection efficiency at NA = 1 (%)	Dipole collection efficiency at NA = 0.42 (%)	Comments
913.8	5645	11.2	80.6	74.1	Perfectly vertical walls
912.9	5109	13.6	79.6	66.8	Perfectly vertical walls + AlGaAs layers oxidized to 200 nm
914.4	4620	8.9	64	61.3	Wall inclination angle of 3.5°
912.9	4965	12	78.2	63.9	Perfectly vertical walls + AlGaAs layers oxidized to 200 nm + protective polyamide
913.8	5633	10.6	84	78.2	Perfectly vertical walls + polyamide on the side
914.4	4572	8.6	67	63.2	Wall inclination angle of 3.5° + protective polyamide

61%, a decrease in the Purcell factor F_P to 8.9, and an increase in the wavelength of radiation by 1 nm because of an increase in V_m of the micropillar. The optically transparent protective polyamide coating with a refractive index of 1.5 for considered CMPs does not significantly worsen the main optical characteristics. The optical characteristics of the CMP with vertical walls and the protective polyamide coating only on the side surfaces of the micropillar are close to the ideal case; their long-term stability can be expected because oxidation is absent.

To summarize, the optical characteristics of cylindrical micropillars with AlGaAs distributed Bragg reflectors and InAs/GaAs quantum dots have been experimentally studied and numerically simulated. The measured spectra of optical reflection from planar micropillar heterostructures have been used to refine the temperature dependences of the refractive indices of used materials that ensure the necessary accuracy of simulation at cryogenic temperatures. The effect of the inclination of sidewalls, the partial oxidation of AlGaAs layers, and the position of the quantum dot with respect to the central axis of the micropillar on the main optical characteristics of the cylindrical micropillar emitting at a wavelength of 920 nm at cryogenic temperatures has been analyzed quantitatively. It has been shown that the Purcell factor and the upward emitted dipole radiation fraction for cylindrical micropillars with a sidewall inclination angle of 0° (perfectly vertical walls) to 3.5° are no less than 80% of their maximum values if the emitted quantum dot does not deviate from the vertical axis of the micropillar by more than 0.4 μm. It has been demonstrated that optically transparent polyamide can be used without significant worsening of the main optical characteristics as a protective coating of sidewalls to fabricate single-photon sources based on cylindrical micropillars with stable characteristics.

FUNDING

The experimental studies on the fabrication of cylindrical vertical micropillars for single-photon sources performed by N.A. Maleev, A.G. Kuz'menkov, A.A. Blokhin, A.P. Vasil'ev, Yu.A. Guseva, M.V. Rakhlin, A.I. Galimov, Yu.M. Serov, S.I. Troshkov, and A.A. Toropov were supported by the State Atomic Energy Corporation Rosatom (contract no. 868-1.3-15/15-2021 dated Oct. 5, 2021, and contract no. R2152 dated Nov. 19, 2021, road map Quantum Computing).

The numerical simulation of optical characteristics of cylindrical vertical micropillars carried out by M.A. Bobrov and V.M. Ustinov was supported by the Ministry of Science and Higher Education of the Russian Federation (agreement no. 075-15-2021-1333 on Sept. 30, 2021, strategic academic leadership program Priority-2030).

The experimental studies of the characteristic of cylindrical vertical micropillars performed by M.V. Rakhlin were supported by the Council of the President of the Russian Federation for State Support of Young Scientists and Leading Scientific Schools.

The analysis of the optical characteristics of cylindrical micropillars with InAs/GaAs quantum dots carried out by S.A. Blokhin was supported by the Russian Foundation for Basic Research together with Deutsche Forschungsgemeinschaft (project no. 20-52-12006).

CONFLICT OF INTEREST

The authors declare that they have no conflicts of interest.

REFERENCES

1. N. Gisin, G. Ribordy, W. Tittel, and H. Zbinden, Rev. Mod. Phys. **74**, 145 (2002). https://doi.org/10.1103/RevModPhys.74.145
2. E. Knill, R. Laflamme, and G. J. Milburn, Nature (London, U.K.) **409**, 46 (2001). https://doi.org/10.1038/35051009
3. A. K. Verma, F. Bopp, J. J. Finley, B. Jonasa, A. Zrennera, and D. Reutera, J. Cryst. Growth **15**, 126715 (2022). https://doi.org/10.1016/j.jcrysgro.2022.126715
4. Y. Marzin, J.-M. Gérard, A. Izrael, D. Barrier, and G. Bastard, Phys. Rev. Lett. **73**, 716 (1994). https://doi.org/10.1103/PhysRevLett.73.716
5. Y.-L. D. Ho, T. Cao, P. S. Ivanov, M. J. Cryan, I. J. Craddock, C. J. Railton, and J. G. Rarity, IEEE J. Quantum Electron. **43**, 1558 (2007). https://doi.org/10.1109/JQE.2007.897905
6. Y. Horikoshi, *General Description of MBE* (Waseda Univ., Tokyo, 2019). https://doi.org/10.1002/9781119354987.CH2
7. L. Sapienza, M. Davanc, A. Badolato, and K. Srinivasan, Nat. Commun. **6**, 7833 (2015). https://doi.org/10.48550/arXiv.1503.07141
8. A. I. Galimov, M. V. Rakhlin, G. V. Klimko, Yu. M. Zadiranov, Yu. A. Guseva, S. I. Troshkov, T. V. Shubina, and A. A. Toropov, JETP Lett. **113**, 252 (2021). https://doi.org/10.1134/S0021364021040093
9. S. Li, Y. Chen, X. Shang, Y. Yu, J. Yang, J. Huang, X. Su, J. Shen, B. Sun, H. Ni, X. Su, K. Wang, and Z. Niu, Nanoscale Res. Lett. **15**, 145 (2020). https://doi.org/10.1186/s11671-020-03358-1
10. X. Ding, Y. He, Z. C. Duan, N. Gregersen, M. C. Chen, S. Unsleber, S. Maier, C. Schneider, M. Kamp, S. Höfling, C.-Y. Lu, and J.-W. Pan, Phys. Rev. Lett. **116**, 020401 (2016). https://doi.org/10.1103/PhysRevLett.116.020401
11. J. Talghader and J. S. Smith, Appl. Phys. Lett. **66**, 335 (1995). https://doi.org/10.1063/1.114204
12. A. Taflove and S. H. Hagness, *Computational Electrodynamics: The Finite Difference Time-Domain Method* (Artech House, Boston, 2005).
13. W. Yu and R. Mittra, IEEE Microw. Wireless Compon. Lett. **11**, 25 (2011). https://doi.org/10.1109/7260.905957
14. E. M. Purcell, Phys. Rev. **69**, 681 (1946). https://doi.org/10.1103/PhysRev.69.674.2
15. O. Gazzano, S. Michaelis de Vasconcellos, C. Arnold, A. Nowak, E. Galopin, I. Sagnes, L. Lanco, A. Lemaître, and P. Senellart, Nat. Commun. **4**, 1425 (2012). https://doi.org/10.1038/ncomms2434

Translated by R. Tyapaev